BIOCHEMICAL PHARMACOLOGY 72 (2006) 749–760

available at www.sciencedirect.com

ScienceDirect

journal homepage: www.elsevier.com/locate/biochempharm

Effective attenuation of acute lung injury in vivo and the formyl peptide-induced neutrophil activation in vitro by CYL-26z through the phosphoinositide 3-kinase γ pathway

Yu-Hsiang Kuan [a], Ruey-Hseng Lin [b], Yeh-Long Chen [c], Lo-Ti Tsao [a], Cherng-Chyi Tzeng [c], Jih-Pyang Wang [a,d,*]

[a] Department of Education and Research, Taichung Veterans General Hospital, Taichung 407, Taiwan, ROC
[b] Institute of Medicine and Department of Pharmacology, Chung Shan Medical University, Taichung 402, Taiwan, ROC
[c] Faculty of Medicinal and Applied Chemistry, College of Life Science, Kaohsiung Medical University, Kaohsiung 807, Taiwan, ROC
[d] Graduate Institute of Pharmaceutical Chemistry, China Medical University, Taichung 404, Taiwan, ROC

ARTICLE INFO

Article history:
Received 25 April 2006
Accepted 9 June 2006

Keywords:
CYL-26z
Acute lung injury
Neutrophils
Chemotaxis
Respiratory burst
Ras
PI3Kγ

Abbreviations:
ALI, acute lung injury
BAL, bronchoalveolar lavage
CYL-26z, 5-[4-acridin-9-ylamino]phenyl]-5-methyl-3-methylenedihydrofuran-2-one
ERK, extracellular signal regulated kinase
fMLP, formyl-Met-Leu-Phe
HBSS, Hanks' balanced salt solution
LPS, lipopolysaccharide
MAPK, mitogen-activated protein kinase

ABSTRACT

5-[4-Acridin-9-ylamino]phenyl]-5-methyl-3-methylenedihydrofuran-2-one (CYL-26z) inhibited the polymorphonuclear leukocyte (PMNL) infiltration and protein leakage into the lungs in lipopolysaccharide (LPS)-induced acute lung injury (ALI) in mice as determined on the basis of PMNL and protein contents in bronchoalveolar lavage (BAL) fluid and myeloperoxidase (MPO) content in whole lung extracts. CYL-26z also attenuated the formyl-Met-Leu-Phe (fMLP)-induced neutrophil chemotaxis and respiratory burst in vitro (IC_{50} 8.4 ± 0.9 μM and 2.0 ± 0.6 μM, respectively). CYL-26z had no effect on superoxide anion ($O_2^{\bullet-}$) generation during dihydroxyfumaric acid autoxidation or on the NADPH oxidase activity in two cell-free systems (the arachidonic acid-induced assembly of NADPH oxidase and the preassembled oxidase caused by phorbol ester treatment), whereas it inhibited NaF-induced respiratory burst. Inhibition of respiratory burst by CYL-26z was readily reversible by washing. Only slight, but significant, inhibition of extracellular signal regulated kinase (ERK) phosphorylation and p38 mitogen-activated protein kinase (MAPK) activation in response to fMLP by CYL-26z up to 30 μM was obtained. CYL-26z effectively blocked the formation of phosphatidylinositol-3,4,5-trisphosphate (PtdIns(3,4,5)P_3) as determined by immunofluorescence microscopy and flow cytometry assays and the dual phosphorylation of protein kinase B (PKB/Akt) on S473 and T308 residues in fMLP-stimulated neutrophils. The membrane recruitment of p110γ and Ras, the Ras activation, and the association between p110γ and Ras were also attenuated by CYL-26z. These results indicate that the blockade of Ras activation by CYL-26z attenuated the downstream phosphoinositide 3-kinase (PI3K) γ signaling, which is involved in chemoattractant-induced neutrophil chemotaxis and respiratory burst, and may have a beneficial anti-inflammatory effect on ALI.

* *Corresponding author*. Tel.: +886 4 2359 2525x4023; fax: +886 4 2359 2705.
E-mail address: w1994@vghtc.gov.tw (J.-P. Wang).
0006-2952/$ – see front matter
doi:10.1016/j.bcp.2006.06.025

MAPKAPK-2, MAPK-activated protein kinase-2
MPO, myeloperoxidase
$O_2^{\bullet-}$, superoxide anion
PDK, 3′-phosphoinositide-dependent kinase
PI3K, phosphoinositide 3-kinase
PKB/Akt, protein kinase B
PMA, phorbol 12-myristate 13-acetate
PtdIns(3,4,5)P_3, phosphatidylinositol-3,4,5-trisphosphate

1. Introduction

Neutrophils are cells of the innate immune system, which are recruited to sites of acute inflammation in response to chemoattractants. Most chemoattractants bind to a G_i-coupled receptor to elicit a range of responses in leukocytes including chemotaxis and respiratory burst [1]. Chemotaxis is a complex process that involves the functional coordination of a diverse array of proteins to induce morphological changes characterized by cell elongation and formation of lamellae at the leading edge and to produce cellular movement via rearrangements of the actin cytoskeleton [2]. The recruitment of neutrophils into inflamed tissues is dependent upon a series of sequential adhesive events that occur between neutrophils and the microvasculature. This includes up-regulation of adhesion molecules on the luminal surface of blood vessels and on the circulating neutrophils to promote rapid attachment and rolling of these cells in preparation for transendothelial migration toward inflammatory foci [3]. However, the abnormal accumulation of neutrophils has implicated in several diseases.

The rapid accumulation of neutrophils in the lung in response to inflammatory stimuli is one of the first recognizable events and plays a critical role in the pathogenesis of many pulmonary diseases such as acute lung injury (ALI) and acute respiratory distress syndrome [4], through the release of reactive oxygen species and lysosomal enzymes. These pulmonary diseases are clinical syndromes characterized by an excessive inflammatory response that ultimately leads to a disruption of alveolar-capillary integrity with severe consequences for pulmonary gas exchange. At present, no specific therapy is available for these syndromes. The process by which neutrophils cross the pulmonary vasculature, migrate through the lung interstitium, and ultimately accumulate in the airways requires complex interactions between circulating leukocytes and the cells of the lung [5]. Although interactions between leukocytes and endothelium have been well characterized in the systemic microcirculation, molecular requirements in the lung are not well defined yet.

5-[4-Acridin-9-ylamino]phenyl]-5-methyl-3-methylenedihydrofuran-2-one (CYL-26z) has been found to inhibit phospholipase D activity through the blockade of RhoA activation in rat neutrophils [6] and to down-regulate the tumor necrosis factor-α-induced intercellular adhesion molecule-1 (ICAM-1) expression through suppression of IκB kinase activity and NF-κB activation in human A549 alveolar epithelial cells and the adhesion of human U937 monocytic leukemia cells to A549 cells [7]. Since the reorganization of actin filament to formation of the leading edge in neutrophils is modulated by Rho family G proteins [8] and by the participation of ICAM in the recruitment of neutrophils to the endothelium [3], we decided to investigate the in vivo as well as in vitro effect of CYL-26z on neutrophil chemotaxis in the present study.

2. Materials and methods

2.1. Materials

Dextran T-500, enhanced chemiluminescence reagent, and protein A agarose beads were purchased from Amersham Pharmacia Biotech. Hanks' balanced salt solution (HBSS) and calcein-AM were obtained from Invitrogen. Mouse monoclonal PtdIns(3,4,5)P_3 antibody was obtained from Echelon Research Laboratories. Rabbit polyclonal antibodies to Akt1/2, CD88, and goat polyclonal p110γ antibodies were obtained from Santa Cruz Biotechnology. Rabbit polyclonal antibodies to phospho-p44/42 MAPK, phospho-p38 MAPK, phospho-Akt(S473) and phospho-Akt(T308) were purchased from Cell Signaling Technology. Mouse monoclonal GST antibody was obtained from Abcam. Secondary antibodies were obtained from Jackson ImmunoResearch Laboratories. 2-(4-Morpholinyl)-8-phenyl-4*H*-1-benzopyran-4-one (LY 294002) and 4-(4-fluorophenyl)-2-(4-methylsulfinylphenyl)-5-(4-pyridyl)-1*H*-imidazole (SB 203580) were obtained from Calbiochem-Novabiochem. Polyvinylidene difluoride membrane was obtained from Millipore. Ras activation assay kit was purchased from Upstate. Liu's stain kit was purchased from Tonyar Biotechnology (Taiwan). FluoroBlok™ Insert System was obtained from BD Biosciences. Other chemicals were purchased from Sigma–Aldrich. CYL-26z (purity > 99%) was dissolved in dimethyl sulfoxide (DMSO). The final volume of DMSO in the reaction mixture was <0.5%.

2.2. Murine model of ALI

BALB/c mice (20–25 g), obtained from the National Laboratory Animal Center (Taiwan), were divided into five experimental groups. CYL-26z or vehicle was intraperitoneally administered 0.5 h before a single intratracheal injection of saline (50 μl) or lipopolysaccharide (LPS) (100 μg/50 μl) [9]. Animals received

DMSO followed by saline (group A, $n = 16$) or LPS (group B, $n = 19$) challenge. In other three groups, animals received 3 μmol/kg (group C, $n = 16$), 10 μmol/kg (group D, $n = 18$) or 30 μmol/kg (group E, $n = 18$) of CYL-26z followed by LPS challenge. Six hours after saline or LPS administration, mice were anesthetized with sodium pentobarbital (60 mg/kg, i.p.). The lungs of half of mice in each group were lavaged in situ via tracheal cannula with five 1-ml aliquots of sterile saline. The total cell count and the populations of macrophage and polymorphonuclear leukocytes (PMNLs) (in a total of 200 cells) in bronchoalveolar lavage (BAL) were determined. Protein concentrations in the cell-free BAL were determined using Bio-Rad protein assay reagents. A standard curve was generated in the same fashion using bovine serum albumin. The lungs of the rest of the mice in each group were isolated and homogenized in 0.1 M phosphate buffer (pH 7.0) supplemented with 0.5% cetyltrimethylammonium bromide for myeloperoxidase (MPO) analysis [10]. Briefly, the supernatant was added into a 1.5 ml phosphate buffer containing 0.2% cetyltrimethylammonium bromide in the presence of 10 mM guaiacol. Reaction was stated by the addition of 0.01% H_2O_2 and the absorbance change was monitored at 470 nm. All experiments were approved by the Institutional Animal Ethics Committee and conducted in accordance with the principles and guideline of the U.S. National Institute of Health Guide for the Care and Use of Laboratory Animals.

2.3. Isolation of neutrophils

Rat (Sprague–Dawley, 350–400 g) blood was collected from the abdominal aorta and the neutrophils were purified by dextran sedimentation, centrifugation through Ficoll-Paque, and hypotonic lysis of erythrocytes [11]. Purified neutrophils containing >95% viable cells were resuspended in HBSS containing 10 mM HEPES, pH 7.4, and 4 mM $NaHCO_3$, and kept in an ice bath before use.

2.4. Chemotaxis assay

Neutrophils chemotaxis was performed by FluoroBlok Insert Systems according to the instructions of the manufacturer. Briefly, neutrophils (10^7 cells) were incubated with 5 μM calcein-AM for 15 min at 37 °C. After being washed, cells were resuspended in HBSS containing 1% bovine serum albumin. Calcein-loaded cells were placed in FluoroBlok Inserts in the presence or absence of 0.1 μM formyl-Met-Leu-Phe (fMLP). Chemotaxis was measured by detecting the fluorescence of cells migrating through the pores (3 μm) to the lower chamber. Fluorescence changes, termed as relative fluorescence units (RFUs), were monitored with a fluorescence microplate reader at 485/530 nm.

2.5. Measurement of superoxide anion ($O_2^{\bullet-}$) generation

Neutrophil $O_2^{\bullet-}$ generation was determined by the superoxide dismutase-inhibitable reduction of ferricytochrome *c* [11]. Briefly, the assay mixture contained neutrophil suspension (2×10^6 cells) and 40 μM of ferricytochrome *c* in a final volume of 1.5 ml. For the determination of $O_2^{\bullet-}$ scavenging activity, the $O_2^{\bullet-}$ generation in a cell-free system was assessed by measuring the reduction of nitroblue tetrazolium during dihydroxyfumaric acid (1.78 mM) autoxidation. Absorbance changes in the reduction of ferricytochrome *c* and nitroblue tetrazolium were monitored continuously at 550 and 560 nm, respectively, in a double-beam spectrophotometer.

2.6. Measurement of NADPH oxidase activity in cell-free systems

Neutrophils (1×10^8 cells) were treated with 2.5 mM diisopropyl fluorophosphate, then disrupted in Tris buffer by sonication, and fractionated by centrifugation as described previously [11]. Briefly, supernatants were pooled as the cytosolic fractions. Pellets were collected and resuspended in Tris buffer as the membrane fractions. Plasma membrane and cytosolic fractions were mixed in 1.5 ml of assay buffer (0.17 M sucrose, 2 mM NaN_3, 1 mM $MgCl_2$, 1 mM EGTA, 65 mM KH_2PO_4–NaOH, pH 7.0) supplemented with 10 μM FAD, 3 μM GTPγS, 0.25 mg/ml of ferricytochrome *c*, 50 μM NADPH, and activated by 100 μM arachidonic acid. Phorbol 12-myristate 13-acetate (PMA)-activated NADPH oxidase was isolated and the activity was determined as described previously [11]. Briefly, the assay mixture contained 0.04% (w/v) sodium deoxycholate, 12.5 μM FAD, 0.25 mg/ml of ferricytochrome *c*, particulate protein solution, and 62.5 μM NADPH in a final volume of 1.6 ml. NADPH oxidase activity was measured spectrophotometrically by continuous detection of the absorbance changes of superoxide dismutase-inhibitable ferricytochrome *c* reduction at 550 nm.

2.7. Immunoblot analysis of protein phosphorylation

The reactions of neutrophil (2×10^7 cells) suspension were terminated by the addition of a stop solution containing 20% (w/v) trichloroacetic acid, 1 mM phenylmethylsulphonyl fluoride, 2 mM *N*-ethylmaleimide, 10 mM NaF, 2 mM Na_3VO_4, 2 mM *p*-nitrophenyl phosphate, and 10 μg/ml each of leupeptin and pepstatin A. Proteins (60 μg per lane) were resolved by 10% SDS-PAGE (for MAPK) or 7.5% SDS-PAGE (for PKB/Akt), and then transferred to polyvinylidene difluoride membrane [11]. The membranes were blocked with 5% (w/v) nonfat dried milk and probed with anti-phospho-p38 MAPK, anti-phospho-MAPKAPK-2, anti-phospho-Akt(S473) or anti-phospho-Akt(T308) antibodies. The blots were then stripped and reprobed with anti-p38 MAPK or anti-Akt antibody to standardize protein loading. Detection was performed with the enhanced chemiluminescence reagent. Quantification was by Luminescent Image Analyzer (Fujifilm LAS-3000).

2.8. Detection of phosphatidylinositol-3,4,5-trisphosphate (PtdIns(3,4,5)P_3) formation by immunofluoroscence microscopy and by flow cytometry

Neutrophils (5×10^5 cells) were fixed with 4% paraformaldehyde in TBS (150 mM NaCl, and 10 mM Tris–HCl, pH 7.5) and plated onto poly-L-lysine coated coverslips. Cells were then thoroughly washed twice and permeabilized with saponin solution (0.2% saponin, 100 mM NaCl, 10 mM Tris–HCl, pH 7.5, 2% fetal bovine albumin, and 1% bovine serum albumin) at room temperature for 30 min. After blocking with 10% bovine serum albumin, anti-PtdIns(3,4,5)P_3 antibody was added and incubated at 4 °C overnight. Cells were then washed three

times with TBS, and rhodamine-labeled anti-mouse IgM antibody was added and incubated at room temperature for 30 min. The fluorescence in the cells was observed using a confocal laser-scanning microscope (Leica TCS NT).

After fixation, permeabilization and blocking of neutrophils with 2% bovine serum albumin, anti-PtdIns(3,4,5)P_3 antibody was added and incubated for 2 h at room temperature. After being washed with TBS, the secondary antibody was added and incubated at room temperature for 1 h and counted on a FACSCalibur flow cytometry system in both side and forward scatter using Cell-FIT software. The mean fluorescence intensity (MFI) of the control group was subtracted from the MFI of the specific antibody-treated groups.

2.9. Membrane association of p110γ and Ras

Neutrophils (2×10^7 cells/ml) were suspended in ice-cold extraction buffer (50 mM Tris–HCl, pH 7.5, 2 mM EGTA, 50 mM 2-mercaptoethanol, 1 mM phenylmethylsulphonyl fluoride, 1 mM benzamidine, and 10 μg/ml each of aprotinin, leupeptin and pepstatin A). After sonication, the lysates were centrifuged (800 × *g* for 10 min at 4 °C) to remove the unbroken cells and nuclei, and then further centrifuged (150,000 × *g* for 90 min at 4 °C) to collect pellets as membrane fractions. Proteins were resolved by 10% SDS-PAGE (for p110γ) or 15% SDS-PAGE (for Ras), and probed with antibodies against p110γ and Ras, respectively, and also with CD88 antibody to standardize the protein loading.

2.10. Ras activation assay

Ras activation was determined by using a Ras activation assay kit according to the instructions of the manufacturer. Neutrophils (2×10^7 cells) were washed twice with ice-cold HBSS containing 25 mM NaF and 1 mM Na_3VO_4, and then resuspended in Mg^{2+} lysis/wash buffer (25 mM HEPES, pH 7.5, 150 mM NaCl, 1% Igepal CA-630, 10 mM $MgCl_2$, 1 mM EDTA, 10% glycerol, 10 μg/ml each of aprotinin and leupeptin, 25 mM NaF, and 1 mM Na_3VO_4) on ice for 15 min. After centrifugation (14,000 × *g* for 5 min at 4 °C), the cell lysate was incubated with GST fusion Raf-1 Ras-binding domain (RBD) agarose for 1 h at 4 °C with constant mixing. The beads were then washed three times with lysis buffer and eluted by boiling in Laemmli sample buffer. Ras was detected by immunoblotting with anti-Ras antibody, and the blots above were also probed with antibody against GST to standardize the protein loading in each lane.

2.11. Immunoprecipitation of p110γ

Neutrophils (2×10^7 cells) were suspended in 0.5 ml lysis buffer (50 mM Tris–HCl, pH 8.0, 100 mM NaCl, 1 mM EGTA, 1 mM EDTA, 1% Nonidet P-40 (v/v), 0.05% SDS, 0.5% sodium deoxycholate, 2 mM Na_3VO_4, 1 mM dithiothreitol, and 1 μg/ml each of leupeptin, aprotinin, and pepstatin A) on ice for 30 min [12]. Cell debris was sedimented (12,000 × *g* for 10 min at 4 °C). Lysates (0.5 mg protein) were precleared by incubation with protein A-Sepharose (10 μl of a 1:1 slurry). Supernatants were then incubated with an anti-p110γ antibody for 2 h at 4 °C with constant mixing. Protein A-Sepharose was added and after overnight incubation at 4 °C, the immunocomplexes were sedimented and washed twice with lysis buffer. The samples were then used in Western blot analysis.

2.12. Statistical analysis

Statistical analyses were performed using ANOVA followed by the Bonferroni *t*-test for multigroup comparisons; $p < 0.05$ was considered significant for all tests. The curve estimation regression analysis with logarithmic model (SPSS) was used to calculate IC_{50} values.

3. Results

3.1. Effect of CYL-26z on LPS-induced ALI in murine model

The murine model of ALI, which uses a single intratracheal administration of LPS, the major structural component of the outer wall of gram-negative bacteria, to induce an acute

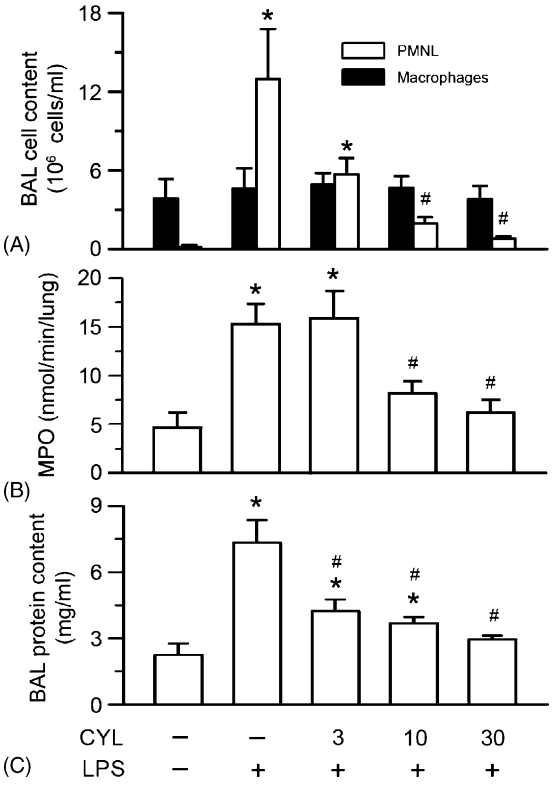

Fig. 1 – Effect of CYL-26z (CYL) on LPS-induced ALI in mice. (A) DMSO or 3–30 μmol/kg of CYL were intraperitoneally injected 0.5 h prior to intratracheal instillation of LPS (100 μg/50 μl saline) or saline in BALB/c mice. Six hours later, half of the mice in each group were anesthetized and used to collect the BAL fluid for PMNL and macrophage count. (B) The lungs of the rest of the mice in each group were removed for the measurement of MPO activity. (C) Lung permeability was determined by quantitating the protein content in the cell-free BAL. Values are means ± S.D. of 8–10 mice per group. *$p < 0.05$, as compared with the corresponding vehicle control values (column 1). #$p < 0.05$, as compared with the corresponding LPS-challenged control values (column 2).

inflammatory response, was designed to study the critical early stages of lung inflammation in which neutrophil recruitment is a central feature [9]. PMNL migration into the lungs in response to LPS was determined on the basis of BAL fluid PMNL content and MPO, an azurophil granule constituent of neutrophils, content in whole lung extracts. A significant increase was found in PMNL, but not macrophages, and MPO contents from mice 6 h after airway instillation of LPS, which is in line with the results of previous reports [13,14]. Pretreatment of mice with CYL-26z evoked a dose-dependent attenuation of both responses (Fig. 1A and B), and a statistical significance began at 3 and 10 μmol/kg of CYL-26z for PMNL and MPO contents, respectively. Moreover, after LPS challenge, protein levels in the cell-free BAL as an index of vascular leakage were significantly increased compared with uninjured (control) lungs (Fig. 1C). This response was also attenuated by CYL-26z in a dose-dependent manner. CYL-26z might have beneficial anti-inflammatory effects on ALI as evidenced from the parallelism of the inhibition of both PMNL influx and protein leakage into the lung.

3.2. *Effect of CYL-26z on neutrophil chemotaxis*

Since neutrophils infiltrate into the lung via chemotaxis, we next examined the effect of CYL-26z on neutrophil chemotaxis in vitro. Addition of chemoattractant fMLP, which activates G protein-coupled receptor, significantly evoked calcein-loaded neutrophils migrating from the FluoroBlok Inserts to the lower chamber as assessed by detecting the increase in fluorescence intensity. This response was attenuated by SB 203580 (30 μM), the p38 mitogen-activated protein kinase (MAPK) inhibitor, and LY 294002 (30 μM), the phosphoinositide 3-kinase (PI3K) inhibitor, and by CYL-26z in a concentration-dependent manner with an IC_{50} value of 8.4 ± 0.9 μM (Fig. 2A). Cell

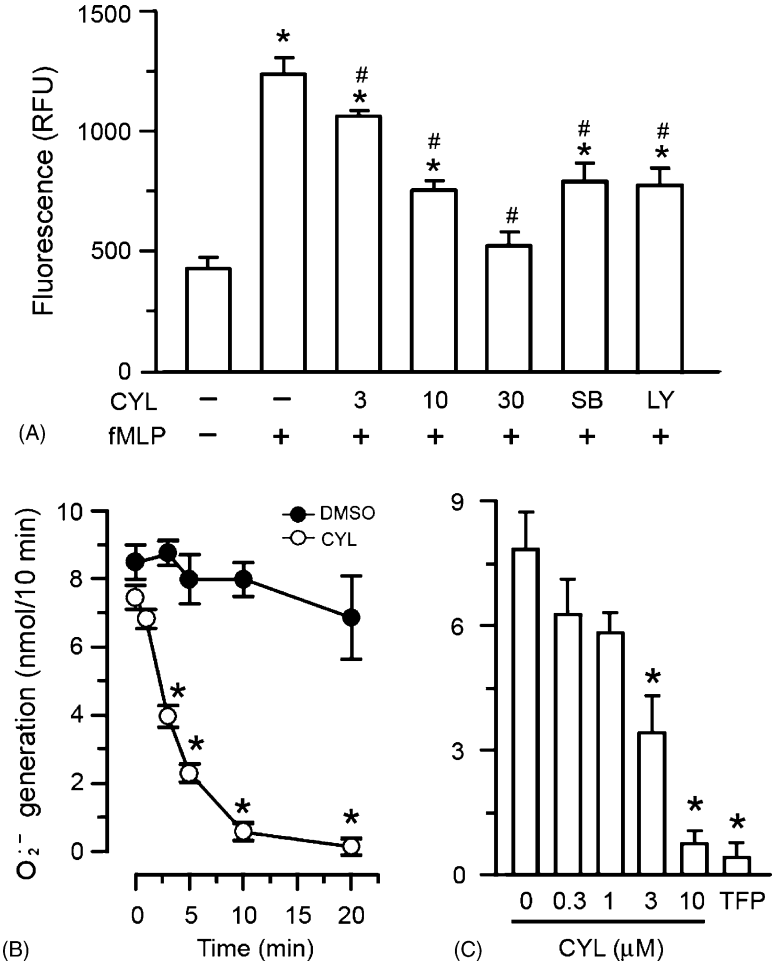

Fig. 2 – Effects of CYL-26z (CYL) on chemotaxis and respiratory burst in fMLP-stimulated neutrophils. (A) Calcein-loaded cells were incubated with DMSO, 3–30 μM CYL, 30 μM SB 203580 (SB) or 30 μM LY 294002 (LY) for 10 min. Cell were then placed in FluoroBlok Inserts in the presence or absence of 0.1 μM fMLP for 2 h. The fluorescence intensity was determined. Values are expressed as means ± S.D. of four independent experiments. $^{*}p < 0.05$, as compared with the vehicle control values (column 1). $^{\#}p < 0.05$, as compared with the activated control values (column 2). Cells were preincubated (B) with DMSO or 10 μM CYL for the indicated time, or (C) with DMSO, 0.3–10 μM CYL for 10 min, or 1 μM trifluoperazine (TFP) for 3 min in the presence of dihydrocytochalasin B (5 μg/ml) before stimulation with 1 μM fMLP. The $O_2^{\bullet-}$ generation was then determined. Values are expressed as means ± S.D. of 4–5 independent experiments. $^{*}p < 0.05$, as compared with the corresponding vehicle control values.

viability was >95% during the incubation with 30 μM CYL-26z at 37 °C for 20 min [6] as well as for 2 h (assessed by trypan blue exclusion and lactate dehydrogenase release). Thus the inhibition of neutrophil chemotaxis may account for the attenuation of neutrophil infiltration into the lung.

3.3. *Effect of CYL-26z on $O_2^{\bullet-}$ generation*

Lung injury is related to the production of reactive oxygen species [15], which play a key role in microvascular permeability in acute inflammation. Activated neutrophils release reactive oxygen species ($O_2^{\bullet-}$ and its metabolites) through NADPH oxidase [16], which catalyzes the reduction of extracellular O_2. This O_2 consumption process is termed respiratory burst. Stimulation of neutrophils with 1 μM fMLP evoked a rapid and transient $O_2^{\bullet-}$ generation, which was abolished by pretreatment of cells with 1 μM trifluoperazine, the NADPH oxidase inhibitor. CYL-26z caused a time-dependent inhibition of $O_2^{\bullet-}$ generation in response to fMLP, significant inhibition was detected at 3 min (54.7 ± 4.2%, $p < 0.05$) and maximal inhibition was detected after 10 min pretreatment (Fig. 2B). CYL-26z also resulted in a concentration-dependent inhibition of $O_2^{\bullet-}$ generation with an IC_{50} value of 2.0 ± 0.6 μM (Fig. 2C). The lack of difference in the absorbance change between the presence and the absence of 30 μM CYL-26z during $O_2^{\bullet-}$ generation in a dihydroxyfumaric acid autoxidation cell-free system, even though SOD (2.5 μg/ml) completely abolished the $O_2^{\bullet-}$ generation (OD_{560} 0.092 ± 0.005 for control versus 0.002 ± 0.001), preclude the $O_2^{\bullet-}$ scavenging activity of CYL-26z.

Addition of 100 μM arachidonic acid to the mixture of neutrophil membrane and cytosol fractions leads to the assembly of NADPH oxidase [17], whereas the NADPH oxidase is already assembled in a PMA-activated neutrophil particulate NADPH oxidase preparation [18]. In the presence of NADPH the $O_2^{\bullet-}$ generation in both cell-free systems was

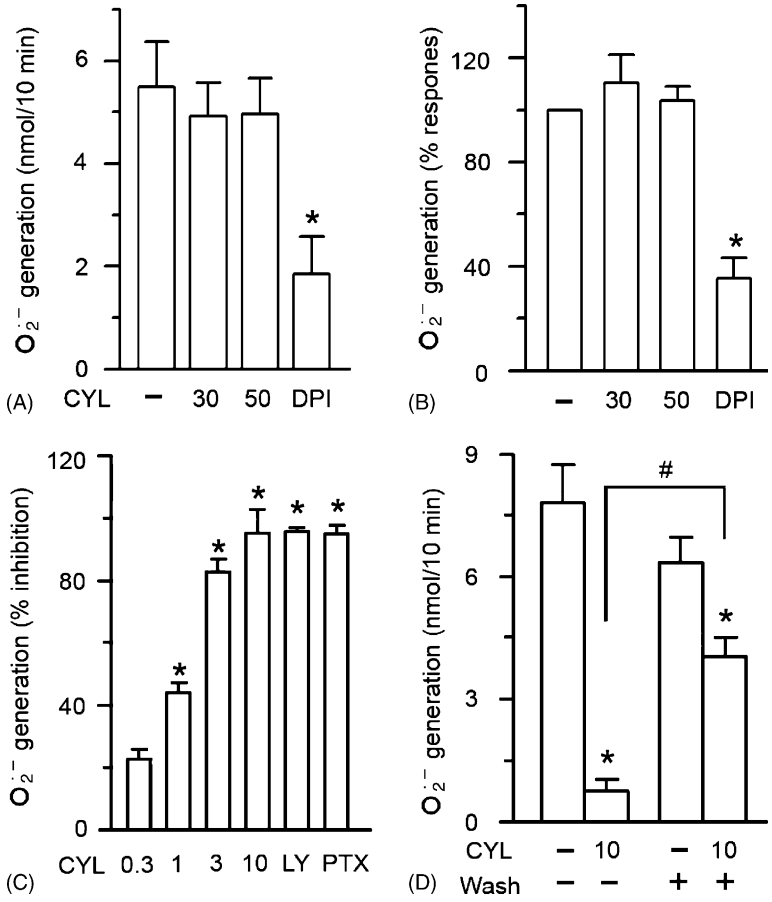

Fig. 3 – Effect of CYL-26z (CYL) on $O_2^{\bullet-}$ generation. (A) The reaction mixtures of neutrophil cytosolic and membrane fractions or (B) the PMA-activated neutrophil particulate NADPH oxidase preparations were preincubated with DMSO, 30 or 50 μM CYL, or 1 μM diphenylene iodonium (DPI) for 10 min, and then NADPH was added in the presence (for A) or absence (for B) of 100 μM arachidonic acid. Values are expressed as means ± S.D. of four independent experiments. $^*p < 0.05$, as compared with the corresponding control values (column 1, 2.6 ± 1.2 nmol $O_2^{\bullet-}$/10 min for B). (C) Neutrophils were pretreated with DMSO (as control), 0.3–10 μM CYL or 30 μM LY 294002 (LY) for 10 min, or with 1 μg/ml of pertussis toxin (PTX) for 1 h before stimulation with 10 mM NaF. Values are expressed as means ± S.D. of 4–5 independent experiments. $^*p < 0.05$, as compared with the control values (5.2 ± 1.1 nmol $O_2^{\bullet-}$/10 min). (D) Neutrophils were incubated with DMSO (as control) or 10 μM CYL for 10 min before being washed twice or not being washed, then stimulated with 1 μM fMLP in the presence of dihydrocytochalasin B (5 μg/ml). Values are expressed as means ± S.D. of 4–5 independent experiments. $^*p < 0.05$, as compared with the corresponding control values. $^\#p < 0.05$.

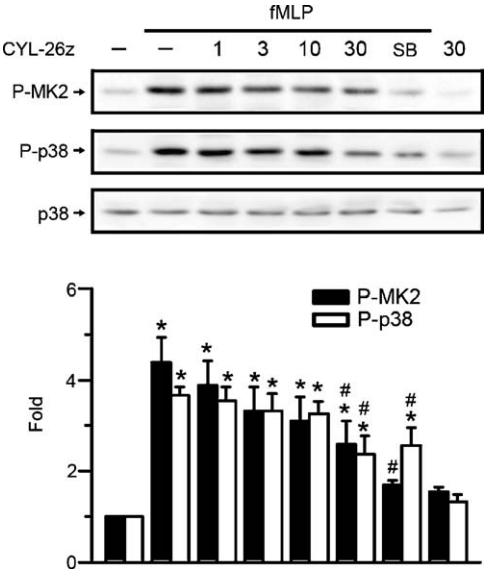

Fig. 4 – Effect of CYL-26z (CYL) on p38 MAPK activation in fMLP-stimulated neutrophils. Cells were preincubated with DMSO, 1–30 μM CYL or 30 μM SB 203580 (SB) for 10 min in the presence of dihydrocytochalasin B (5 μg/ml) before stimulation or no stimulation with 1 μM fMLP for 1 min. Cell lysates were immunoblotted with anti-phospho-p38 MAPK (P-p38) and anti-phospho-MAPKAPK-2 (P-MK2) antibodies. The blot above was then stripped and reprobed with anti-p38 MAPK (p38) antibody. The ratio of immunointensity between the p38 and P-p38 or P-MK2 was calculated. Values are expressed as means ± S.D. of 3–4 independent experiments. $^{*}p < 0.05$, as compared with the corresponding control values (lane 1). $^{\#}p < 0.05$, as compared with the corresponding activated control values (lane 2).

abolished by 1 μM diphenylene iodonium, the NADPH oxidase inhibitor, but was not affected by CYL-26z up to 50 μM (Fig. 3A and B), excluding a target role of oxidase for CYL-26z. NaF has been reported to directly activate G protein, bypassing fMLP receptor, and to induce $O_2^{\bullet-}$ generation in neutrophils [19]. This response was nearly abolished by 30 μM LY 294002 and 1 μg/ml of pertussis toxin, a $G_{i/o}$ inhibitor. The ability of CYL-26z (IC_{50} value of 3.4 ± 1.2 μM) to inhibit NaF-induced $O_2^{\bullet-}$ generation (Fig. 3C) supports a post-receptor level of inhibition of signal transduction. The inhibitory effect of CYL-26z on fMLP-induced $O_2^{\bullet-}$ generation in neutrophils was reversed by washing (36.2 ± 4.7% for washing twice versus 90.3 ± 3.9% inhibition) (Fig. 3D).

3.4. *Effect of CYL-26z on MAPK activation*

At least three distinct mammalian MAPKs have been identified, including extracellular signal regulated kinase (ERK), c-Jun NH_2-terminal kinase, and p38 MAPK [20]. p38 MAPK and ERK participate in LPS-induced ALI [21] and in chemoattractant-induced neutrophil chemotaxis and respiratory burst [22,23]. However, the role of ERK is controversial. The requirement of p38 MAPK signaling is supported by the results that SB 203580 inhibited chemotaxis as shown in Fig. 2A and $O_2^{\bullet-}$ generation in our previous report [12]. Activation of p38 MAPK occurs after dual phosphorylation of T/Y residues within the TGY motif by the upstream MAPK kinases [24], which in turn stimulates phosphorylation and activation of its downstream target, MAPK-activated protein kinase-2 (MAPKAPK-2). Stimulation of neutrophils with fMLP results in a rapid phosphorylation of p38 MAPK [25]. CYL-26z had no effect on the phosphorylation of p38 MAPK and MAPKAPK-2, except at the concentration of CYL-26z up to 30 μM (45% and 54% inhibition, respectively) (Fig. 4). A similar inhibitory effect was obtained in ERK phosphorylation (data not shown), obviating the role of MAPK. This notion is in line with a previous report in human A549 alveolar epithelial cells [7].

3.5. *Effects of CYL-26z on protein kinase B (PKB/Akt) phosphorylation and PtdIns(3,4,5)P_3 formation*

PI3K, the lipid kinase that phosphorylates the D-3 position of the inositol ring of phosphoinositides, has been implicated in

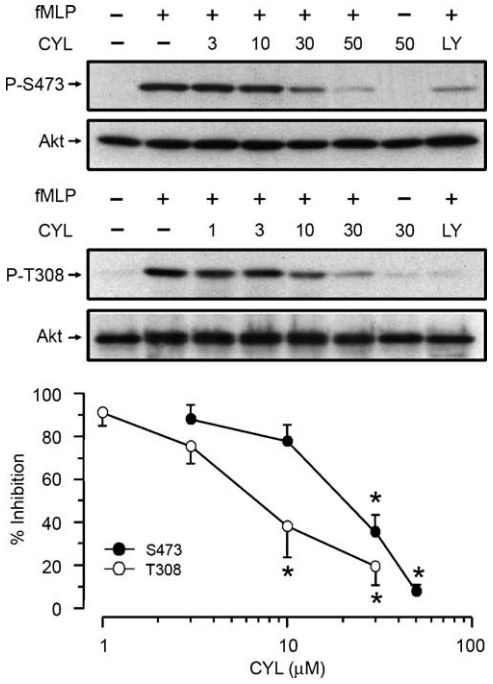

Fig. 5 – Effect of CYL-26z (CYL) on PKB/Akt phosphorylation in fMLP-stimulated neutrophils. Cells were preincubated with DMSO, 1–50 μM CYL or 30 μM LY 294002 (LY) for 10 min in the presence of dihydrocytochalasin B (5 μg/ml) before stimulation or no stimulation with 1 μM fMLP for 1 min. Cell lysates were immunoblotted with anti-phospho-Akt(T308) (P-T308) or anti-phospho-Akt(S473) (P-S473) antibodies. The blots above were then stripped and reprobed with anti-Akt antibody. The ratio of immunointensity between the phospho-Akt and Akt was calculated. Values are expressed as means ± S.D. of 3–4 independent experiments. $^{*}p < 0.05$, as compared with the corresponding activated control values (lane 2, ratio values of 1.10 ± 0.34 for P-S473 and 0.69 ± 0.18 for P-T308, respectively).

LPS-induced ALI [4] and plays a critical role in neutrophil chemotaxis and respiratory burst [26]. This notion is consistent with the results that LY 294002 inhibited chemotaxis as shown in Fig. 2A and respiratory burst in our previous report [27]. PKB/Akt, the effector of PI3K, is activated by ligation of PI3K product, 3-phosphoinositides, and subsequent phosphorylation on both T308 and S473 residues by 3′-phosphoinositide-dependent kinases (PDK) for maximal activation [28]. Stimulation of neutrophils with fMLP results in a rapid phosphorylation of PKB/Akt [27]. CYL-26z inhibited the phosphorylation of both T308 and S473 residues in a concentration-dependent manner with IC_{50} values of 7.5 ± 3.0 μM and 15.7 ± 2.0 μM, respectively (Fig. 5). The parallelism of the inhibition of neutrophil activation and PKB/Akt(T308) phosphorylation by CYL-26z implies a key role for PI3K/Akt signaling.

The cellular PtdIns(3,4,5)P_3 levels, the major product of class I PI3Ks, serve as a convenient marker for PI3K activity and reflect the level of lipid-dependent signaling inside cells. Stimulation of neutrophils with fMLP resulted in PtdIns(3,4,5)P_3 formation that rapidly reached a peak at around 15 s [27]. Pretreatment of cells with CYL-26z resulted in concentration-dependent decrease in PtdIns(3,4,5)P_3 formation, significantly at 3 μM CYL-26z, with an IC_{50} value of 4.9 ± 1.5 μM as assessed by confocal microscopy and flow cytometry (Fig. 6). These results confirm the relevance of PI3K/Akt signaling to the CYL-26z inhibition of neutrophil activation.

3.6. *Effects of CYL-26z on membrane association of PI3Kγ and Ras activation*

PI3Ks are categorized as class I (A and B), II and III, depending on their subunit structure, regulation, and substrate selectivity [29]. Class I has been well characterized, whereas little is known about the functions of class II and III PI3Ks. Class I PI3Ks in resting cells are cytoplasmic proteins. Rat neutrophils express the catalytic subunits of both class IA (p110α, p110β, and p110δ) and IB PI3K (p110γ) [27]. Recent evidence showed that PI3Kγ deficiency impaired the migration of neutrophils in vitro and the infiltration of neutrophils in vivo [30,31] and inhibited neutrophil $O_2^{\bullet-}$ generation [30]. Upon activation, p110γ is recruited into contact with membrane, where its lipid substrates reside [32]. The membrane recruitment of p110γ in response to fMLP is detectable at 5 s and maximal within 15 s [27]. CYL-26z showed a concentration-dependent inhibition of fMLP-induced response with an IC_{50} value of 4.1 ± 1.0 μM (Fig. 7A), suggesting the involvement of PI3Kγ.

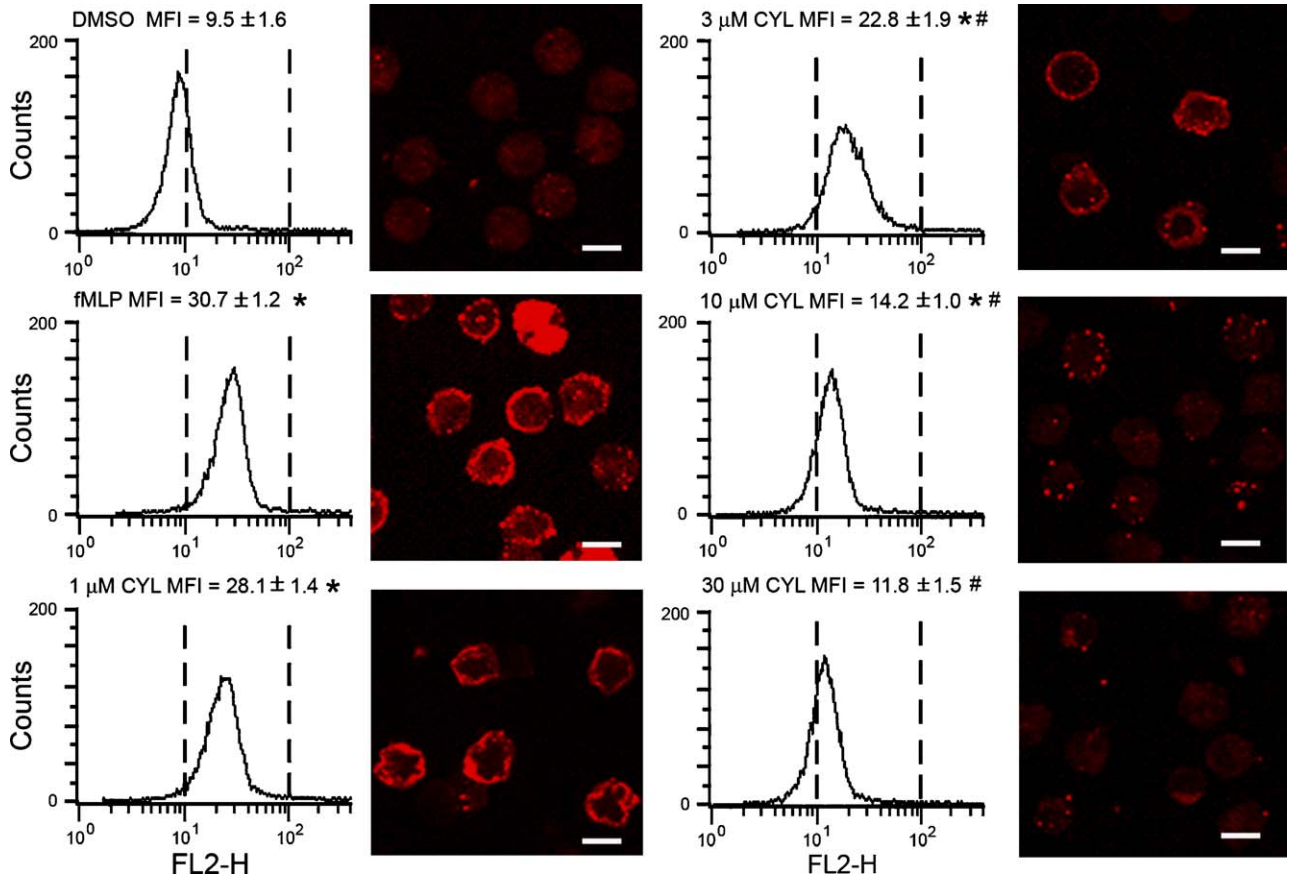

Fig. 6 – Effect of CYL-26z (CYL) on PtdIns(3,4,5)P_3 formation in fMLP-stimulated neutrophils. Cells were incubated with DMSO or 1–30 μM CYL for 10 min in the presence of dihydrocytochalasin B (5 μg/ml) before stimulation or no stimulation with 1 μM fMLP for 15 s. After fixation and permeabilization, cells were probed with anti-PtdIns(3,4,5)P_3 antibody. Samples were counted in flow cytometry and observed by immunofluorescence confocal microscopy (scale bar is 8 μm). Values are expressed as means MFI ± S.D. of 4–5 independent flow cytometry experiments. $^{*}p<0.05$, as compared with the vehicle control value; $^{\#}p < 0.05$, as compared with the activated control value.

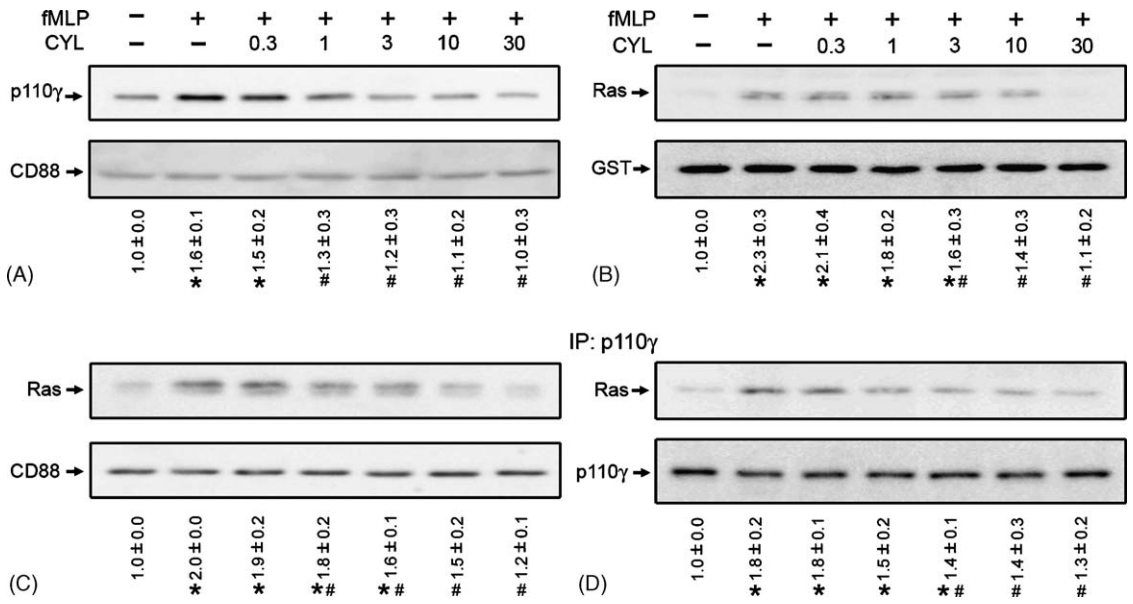

Fig. 7 – Effect of CYL-26z (CYL) on the membrane recruitment of p110γ and Ras activation in fMLP-stimulated neutrophils. Cells were incubated with DMSO or 0.3–30 μM CYL for 10 min in the presence of dihydrocytochalasin B (5 μg/ml) before stimulation with 1 μM fMLP for (A) 15 s, and then the cell membrane fractions were immunoblotted with anti-p110γ antibody, or for (B) 1 min, after which the cell lysates were precipitated with GST fusion Raf-1 RBD agarose, and then immunoblotted with anti-Ras antibody. (C) The cell membrane fractions were immunoblotted with anti-Ras antibody. (D) Cell lysates were immunoprecipitated with anti-p110γ antibody, and then immunoblotted with anti-Ras antibody. The blots above were also probed with anti-CD88, anti-GST or anti-p110γ antibody as the protein loading control. The ratio of immunointensity between the p110γ and CD88 or between the Ras and GST, CD88 or p110γ was calculated. The fold increase in the immunointensity is expressed as means ± S.D. of 4–5 independent experiments. $^{*}p < 0.05$, as compared with the corresponding vehicle control values (lane 1); $^{\#}p < 0.05$, as compared with the activated control values (lane 2).

The p110γ contains Ras-binding domain for GTP form of activated Ras, and signal downstream of Ras [32]. Stimulation of neutrophils with fMLP evoked a rapid Ras activation (assessed by precipitating Ras-GTP with GST-Ras-binding domain agarose) and the recruitment of Ras to membrane [27]. Both responses were concentration-dependently attenuated by CYL-26z with IC_{50} values of 3.6 ± 0.7 μM and 4.5 ± 0.4 μM, respectively (Fig. 7B and C). In addition, the association between Ras and p110γ as assessed by immunoprecipitation with anti-p110γ antibody was inhibited by CYL-26z with an IC_{50} value of 4.2 ± 1.8 μM (Fig. 7D). Thus, the blockade of Ras activation is likely involved in CYL-26z inhibition of PI3Kγ activation.

4. Discussion

In the present study, we found that CYL-26z inhibited PMNL influx and lung permeability in LPS-induced ALI in mice as evidenced from the decrease in PMNL and protein contents in BAL fluid and MPO content in the lung extracts. PMNL recruitment into the lung occurs in a cascade-like sequence of activation, sequestration in pulmonary vessels, transendothelial migration (from blood to interstitium), which is dependent upon a series of sequential adhesive events that occur between PMNL and the microvasculature, and transepithelial migration (from interstitium to alveolar airspace), which requires complex interactions between PMNL and the cells of the lung [33]. In the setting of lung injury, effective migration and accumulation of PMNL into the airspaces requires coordinated responses including up-regulation of adhesion molecules, cytoskeletal rearrangement, increases in cell size and stiffness, and chemotaxis. Each migration step is regulated by distinct adhesion molecules [34]. It is likely that CYL-26z preferentially inhibited the transepithelial rather than transendothelial migration step because a lower dosage was required for inhibition of the PMNL content in BAL fluid than the MPO content in lung extracts. CYL-26z has been reported to suppress the ICAM-1 expression in alveolar epithelial cells in vitro [7]; however, whether this action is also carried on in vivo is far from clear. Further study will be needed to clarify the exact mechanism and the target molecule(s) whereby CYL-26z inhibits PMNL infiltration.

LPS is not an effective chemoattractant for neutrophils in vitro [35], but can trigger an inflammatory cascade via the synthesis of cytokines and other proinflammatory mediators, such as TNF-α and chemokines, by the resident and infiltrated inflammatory cells, which serve to amplify and perpetuate the recruitment of leukocytes to the airspaces, in lung [36]. The combined effects of TNF-α and chemokines on neutrophil recruitment are complex and incompletely understood, including activation of endothelial cells to express adhesion molecules and induction of an array of secondary inflammatory mediators [37]. TNF-α alone does not induce chemotaxis of neutrophils in vitro [38]. We therefore examined the effects of CYL-26z on neutrophil functions in response to fMLP, the

most intensely studied chemoattractants from bacterial proteins. Both PI3K and p38 MAPK signalings have been implicated in LPS-induced ALI [4,21] and in chemoattractant-induced neutrophil chemotaxis [22,26]. The results that SB 203580 and LY 294002 inhibited the fMLP-induced neutrophil chemotaxis are compatible with this notion. Thus the inhibition of neutrophil chemotaxis by CYL-26z may account for the attenuation of PMNL infiltration in ALI.

The multicomponent NADPH oxidase consists of both membrane-bound cytochrome b_{558} ($p22^{phox}$ and $gp91^{phox}$), which contains FAD and heme redox centers, and cytosolic factors ($p40^{phox}$, $p47^{phox}$, $p67^{phox}$ and Rac) in the resting state. These cytosolic factors translocate and interact with cytochrome b_{558} to enter a functional state upon neutrophil activation [16]. Assembly of the oxidase component, probably through conformational change, is essential for the activation of electron flow within cytochrome b_{558}. In the present study, two cell-free NADPH oxidase systems were studied. Protein kinase C, which is directly activated by PMA, plays a role in the phosphorylation of oxidase components and assembly of the active NADPH oxidase complex in the membrane fraction [18]. Addition of arachidonic acid to the cytosolic and membrane fractions mimics the effect of phosphorylation of $p47^{phox}$ upon cell activation, and leads to assembly and activation of NADPH oxidase [17]. CYL-26z attenuated the fMLP- and NaF-induced respiratory burst but had no effect on $O_2^{\bullet-}$ generation in dihydroxyfumaric acid autoxidation and two cell-free NADPH oxidase systems, suggesting interference with the cellular signal transduction step(s) downstream of membrane receptor activation. The parallel inhibition of neutrophil chemotaxis and respiratory burst by CYL-26z implies a beneficial anti-inflammatory effect on ALI.

fMLP stimulates an array of signaling cascades that culminate in the activation of neutrophils, in which phospholipase D, phospholipase C, protein kinase C and Src family tyrosine kinases pathways are essential for $O_2^{\bullet-}$ generation but not required for chemotaxis in neutrophils [30,39-41], whereas p38 MAPK and PI3K pathways play important roles in both responses [22,26]. The results that higher concentration of CYL-26z was required to inhibit the phosphorylation of p38 MAPK and MAPKAPK-2 preclude the involvement of p38 MAPK signaling. The PI3K product, PtdIns(3,4,5)P_3, mediated the recruitment of constitutively active PDK1 and inactive PKB/Akt via the PH domain in both molecules from the cytosol to the plasma membrane, and PKB/Akt was subsequently phosphorylated on T308 by PDK1. Maximal activation of PKB/Akt also requires phosphorylation of S473 in the hydrophobic motif, and phosphorylation by an unidentified kinase called PDK2, the nature of which is controversial [28]. The compelling candidates for PDK2 include rictor-mTOR complex, PDK1, MAPKAPK-2, integrin-linked kinase, PKC-βII, and DNA-dependent protein kinase [42,43]. Both T308 phosphorylation and PtdIns(3,4,5)P_3 formation were attenuated by CYL-26z in a parallel concentration-dependent manner with similar IC_{50} values, whereas inhibition of S473 phosphorylation had a higher IC_{50} value, suggesting that PI3K/PDK1/Akt signaling plays a pivotal role.

In vitro and in vivo studies using PI3Kγ knockout neutrophils demonstrated a major role for the γ isoform in chemotactic events and no other class I PI3K isoform seems to be involved in these chemotactic processes [31]. PI3Kγ consists of the p110γ catalytic subunit complexed to the p101 regulatory subunit, and signals downstream of G protein-coupled receptor and Ras [44]. Upon cell activation, the $G_{\beta\gamma}$-p101 interaction serves to recruit PI3Kγ to the cell membrane, and PI3Kγ activation is the consequence of the interaction of p110γ with $G_{\beta\gamma}$ and active Ras [45]. In the Ras bound structure, the catalytic domain undergoes significant molecular rearrangement that affects the conformation of the phosphoinositide-binding site. The results that the membrane recruitment of p110γ and Ras, the Ras activation, and the association between p110γ and Ras in response to fMLP were effectively attenuated by CYL-26z with IC_{50} values similar to the concentration required for the inhibition of Akt(T308) phosphorylation and PtdIns(3,4,5)P_3 formation support the involvement of Ras/PI3Kγ/Akt signaling pathway.

In conclusion, CYL-26z inhibits PMNL influx into the lungs and lung permeability in LPS-induced ALI in mice and attenuates the neutrophil chemotaxis and respiratory burst in response to fMLP in vitro. These inhibitory effects appear largely attributable to the blockade of PI3Kγ activation via the suppression of Ras activation. Since CYL-26z has been reported to inhibit NF-κB activation in human A549 alveolar epithelial cells [7], we do not exclude the possibility that the anti-inflammatory effects observed in vivo could be also related to the inhibition of local production of inflammatory cytokines and chemokines in the lung. In the present study, we report our efforts to evaluate the compound CYL-26z as a potential candidate for pre-clinical management of ALI. Whether this compound has a beneficial anti-inflammatory effect in the medical management of ALI remains to be investigated.

Acknowledgements

This work was supported by research grants form the National Science Council (NSC-90-2315-B-075A-001) and Taichung Veterans General Hospital (TCVGH-917303C and TCVGH-947316C), Taiwan, Republic of China.

REFERENCES

[1] Murphy PM. The molecular biology of leukocyte chemoattractant receptors. Annu Rev Immunol 1994;12:593–633.
[2] Iijima M, Huang YE, Devreotes P. Temporal and spatial regulation of chemotaxis. Dev Cell 2002;3:469–78.
[3] McEver RP, Moore KL, Cummings RD. Leukocyte trafficking mediated by selectin-carbohydrate interactions. J Biol Chem 1995;270:11025–8.
[4] Abraham E. Neutrophils and acute lung injury. Crit Care Med 2003;31:S195–9.
[5] Worthen GS, Nick JA. Leukocyte accumulation in the lung. In: Fishman AP, editor. Pulmonary diseases and disorders, vol. 1. New York: McGraw-Hill; 1998. p. 325–36.
[6] Kuan YH, Lin RH, Tsao LT, Chen YL, Tzeng CC, Wang JP. Inhibition of phospholipase D activation by CYL-26z in formyl peptide-stimulated neutrophils involves the blockade of RhoA activation. Biochem Pharmacol 2005;70:901–10.

[7] Huang WC, Chan ST, Yang TL, Tzeng CC, Chen CC. Inhibition of ICAM-1 gene expression, monocyte adhesion and cancer cell invasion by targeting IKK complex: molecular and functional study of novel α-methylene-γ-butyrolactone derivatives. Carcinogenesis 2004;25:1925–34.
[8] Niggli V. Signaling to migration in neutrophils: importance of localized pathways. Int J Biochem Cell Biol 2003;35:1619–38.
[9] Yanagihara K, Seiki M, Cheng PW. Lipopolysaccharide induces mucus cell metaplasia in mouse lung. Am J Respir Cell Mol Biol 2001;24:66–73.
[10] Dri P, Cramer R, Soranzo MR, Comin A, Miotti V, Patriarca P. New approaches to the detection of myeloperoxidase deficiency. Blood 1982;60:323–7.
[11] Wang JP, Chang LC, Lin YL, Hsu MF, Chang CY, Huang LJ, et al. Investigation of the cellular mechanism of inhibition of formyl-methionyl-leucyl-phenylalanine-induced superoxide anion generation in rat neutrophils by 2-benzyloxybenzaldehyde. Biochem Pharmacol 2003;65:1043–51.
[12] Kuan YH, Lin RH, Tsao LT, Lin CN, Wang JP. Artocarpol A stimulation of superoxide anion generation in neutrophils involved the activation of PLC, PKC and p38 mitogen-activated PK signaling pathways. Br J Pharmacol 2005;145:460–8.
[13] Corteling R, Wyss D, Trifilieff A. In vivo models of lung neutrophil activation. Comparison of mice and hamsters. BMC Pharmacol 2002;2:1–8.
[14] Speyer CL, Rancilio NJ, McClintock SD, Crawford JD, Gao H, Sarma JV, et al. Regulatory effects of estrogen on acute lung inflammation in mice. Am J Physiol Cell Physiol 2005;288:C881–90.
[15] Pittet JF, Mackersie RC, Martin TR, Matthay MA. Biological markers of acute lung injury: prognostic and pathogenic significance. Am J Respir Crit Care Med 1997;155:1187–205.
[16] Segal AW, Abo A. The biochemical basis of the NADPH oxidase of phagocytes. Trends Biochem Sci 1993;18:43–7.
[17] Fuchs A, Dagher MC, Vignais PV. Mapping the domains of interaction of $p40^{phox}$ with both $p47^{phox}$ and $p67^{phox}$ of the neutrophil oxidase complex using the two-hybrid system. J Biol Chem 1995;270:5695–7.
[18] Majumdar S, Kane LH, Rossi MW, Volpp BD, Nauseef WM, Korchak HM. Protein kinase C isotypes and signal-transduction in human neutrophils: selective substrate specificity of calcium-dependent β-PKC and novel calcium-independent nPKC. Biochim Biophys Acta 1993;1176:276–86.
[19] Strnad CF, Wong K. Calcium mobilization in fluoride activated human neutrophils. Biochem Biophys Res Commun 1985;133:161–7.
[20] Johnson GL, Lapadat R. Mitogen-activated protein kinase pathways mediated by ERK, JNK, and p38 protein kinases. Science 2002;298:1911–2.
[21] Nick JA, Young SK, Brown KK, Avdi NJ, Arndt PG, Suratt BT, et al. Role of p38 mitogen-activated protein kinase in a murine model of pulmonary inflammation. J Immunol 2000;164:2151–9.
[22] Zu YL, Qi J, Gilchrist A, Fernandez GA, Vazquez-Abad D, Kreutzer DL, et al. p38 mitogen-activated protein kinase activation is required for human neutrophil function triggered by TNF-α or FMLP stimulation. J Immunol 1998;160:1982–9.
[23] Kuroki M, O'Flaherty JT. Differential effects of a mitogen-activated protein kinase kinase inhibitor on human neutrophil responses to chemotactic factors. Biochem Biophys Res Commun 1997;232:474–7.
[24] Moriguchi T, Kuroyanagi N, Yamaguchi K, Gotoh Y, Irie K, Kano T, et al. A novel kinase cascade mediated by mitogen-activated protein kinase kinase 6 and MKK3. J Biol Chem 1996;271:13675–9.
[25] Chang LC, Wang JP. Activation of p38 mitogen-activated protein kinase by formyl-methionyl-leucyl-phenylalanine in rat neutrophils. Eur J Pharmacol 2000;390:61–6.
[26] Sasaki T, Irie-Sasaki J, Jones RG, Oliveira-dos-Santos AJ, Stanford WL, Bolon B, et al. Function of PI3Kγ in thymocyte development, T cell activation, and neutrophil migration. Science 2000;287:1040–6.
[27] Kuan YH, Lin RH, Lin HY, Huang LJ, Tasi CR, Tsao LT, et al. Activation of phosphoinositide 3-kinase and Src family kinase is required for respiratory burst in rat neutrophils stimulated with artocarpol A. Biochem Pharmacol 2006;71:1735–46.
[28] Wymann MP, Zvelebil M, Laffargue M. Phosphoinositide 3-kinase signalling-which way to target? Trend Pharmacol Sci 2003;24:366–76.
[29] Deane JA, Fruman DA. Phosphoinositide 3-kinase: diverse roles in immune cell activation. Annu Rev Immunol 2004;22:563–98.
[30] Li Z, Jiang H, Xie W, Zhang Z, Smrcka AV, Wu D. Roles of PLC-2 and -3 and PI3K in chemoattractant-mediated signal transduction. Science 2000;287:1046–9.
[31] Thomas MJ, Smith A, Head DH, Milne L, Nicholls A, Pearce W, et al. Airway inflammation: chemokine-induced neutrophilia and the class I phosphoinositide 3-kinases. Eur J Immunol 2005;35:1283–91.
[32] Vanhaesebroeck B, Leevers SJ, Ahmadi K, Timms J, Katso R, Driscoll PC, et al. Synthesis and function of 3-phosphorylated inositol lipids. Annu Rev Biochem 2001;70:535–602.
[33] Reutershan J, Basit A, Galkina EV, Ley K. Sequential recruitment of neutrophils into lung and bronchoalveolar lavage fluid in LPS-induced acute lung injury. Am J Physiol Lung Cell Mol Physiol 2005;289:L807–15.
[34] Razavi HM, Wang L, Weicker S, Rohan M, Law C, McCormack DG, et al. Pulmonary neutrophil infiltration in murine sepsis: role of inducible nitric oxide synthase. Am J Respir Crit Care Med 2004;170:227–33.
[35] Carroll EJ, Mueller R, Panico L. Chemotactic factors for bovine leukocytes. Am J Vet Res 1982;43:1661–4.
[36] Xing Z, Kirpalani H, Torry D, Jordana M, Gauldie J. Polymorphonuclear leukocytes as a significant source of TNF-α in endotoxin-challenged lung tissue. Am J Pathol 1993;143:1009–15.
[37] Fantone JC. Cytokines and neutrophils: neutrophil-derived cytokines and the inflammatory response. In: Remick DG, Friedland JS, editors. Cytokines in health and disease. New York: Marcel Dekker; 1997. p. 373–80.
[38] Otsuka Y, Nagano K, Nagano K, Hori K, Oh-Ishi J, Hayashi H, et al. Inhibition of neutrophil migration by tumor necrosis factor ex vivo and in vivo studies in comparison with in vitro effect. J Immunol 1990;145:2639–43.
[39] Yasui K, Yamazaki M, Miyabayashi M, Tsuno T, Komiyama A. Signal transduction pathway in human polymorphonuclear leukocytes for chemotaxis induced by a chemotactic factor. Distinct from the pathway for superoxide anion production. J Immunol 1994;152:5922–9.
[40] Ferretti ME, Nalli M, Biondi C, Colamussi ML, Pavan B, Traniello S, et al. Modulation of neutrophil phospholipase C activity and cyclic AMP levels by fMLP-OMe analogues. Cell Signal 2001;13:233–40.
[41] Nijhuis E, Lammers JW, Koenderman L, Coffer PJ. Src kinases regulate PKB activation and modulate cytokine and chemoattractant-controlled neutrophil functioning. J Leukoc Biol 2002;71:115–24.

[42] Sarbassov DD, Guertin DA, Ali SM, Sabatini DM. Phosphorylation and regulation of Akt/PKB by the rictor-mTOR complex. Science 2005;307:1098–101.
[43] Woodgett JR. Recent advances in the protein kinase B signaling pathway. Curr Opin Cell Biol 2005;17:150–7.
[44] Vanhaesebroeck B, Ali K, Bilancio A, Geering B, Foukas LC. Signalling by PI3K isoforms: insights from gene-targeted mice. Trends Biochem Sci 2005;30:194–204.
[45] Koyasu S. The role of PI3K in immune cells. Nat Immunol 2003;4:313–9.